

Rhodium(I) Complexes with Ligands Based on N-Heterocyclic Carbene and Hemilabile Pyridine Donors as Highly *E* Stereoselective Alkyne Hydrosilylation Catalysts

Judith P. Morales-Cerón,[†] Patricia Lara,[‡] Joaquín López-Serrano,[‡] Laura L. Santos,[‡] Verónica Salazar,^{*,†} Eleuterio Álvarez,[‡] and Andrés Suárez^{*,‡}

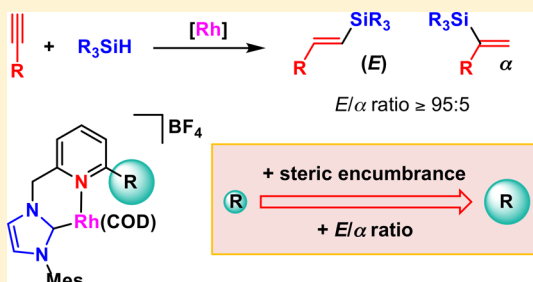
[†]Área Académica de Químicas, Universidad Autónoma del Estado de Hidalgo 42184 Mineral de la Reforma, Hidalgo, Mexico

[‡]Instituto de Investigaciones Químicas (IIQ), Departamento de Química Inorgánica and Centro de Innovación en Química Avanzada (ORFEO-CINQA), CSIC and Universidad de Sevilla, 41092 Sevilla, Spain

Supporting Information

ABSTRACT: Cationic rhodium(I) complexes containing picolyl-NHC (NHC = N-heterocyclic carbene) ligands that differ in the substitution at the 6-position of the pyridine donor serve as efficient *E*-selective alkyne hydrosilylation catalyst precursors. Particularly, when the steric hindrance of the picolyl fragment is increased, a catalyst precursor exhibiting high catalytic activities (TOF up to 500 h⁻¹ at S/C ratios of 1000) and excellent *E* selectivities (*E*/ α ratio $\geq 95/5$) in the hydrosilylation of a series of aryl, alkyl, and functionalized terminal alkynes with both carbo- and alkoxy-silanes has been obtained. The picolyl-NHC ligands in the Rh complexes exhibit a dynamic behavior in solution due to the hemilabile coordination of the pyridine fragment.

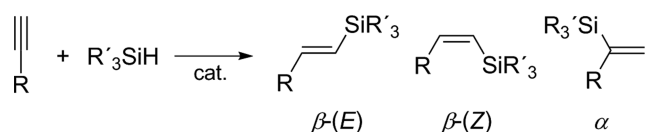
Preliminary mechanistic studies support the involvement of Rh silyl hydrido species, which are generated in low concentrations from Rh complexes and the silane, in the hydrosilylation of alkynes in agreement with the assumption of Chalk–Harrod-type mechanisms.



INTRODUCTION

Vinylsilanes are widely employed reactants in organic synthesis that can be conveniently accessed by the atom-economical, metal-catalyzed hydrosilylation of alkynes.^{1,2} Although transition-metal catalysts for the addition of hydrosilanes to alkynes have been known for a long time, the search for active and, more importantly, selective catalysts still represents a challenge. For example, with respect to the selectivity issue, hydrosilylation of terminal alkynes produces up to three stereoisomers, namely β -(*Z*), β -(*E*), and α isomers (Scheme 1).

Scheme 1. Hydrosilylation of Terminal Alkynes



Among the various catalysts employed for alkyne hydrosilylation, those based on Pt give predominantly β -(*E*)-alkenylsilanes,³ while the β -(*Z*) or α isomers are preferentially formed when Ru catalysts are employed.^{4,5} Other catalytic systems, such as those based on Ir⁶ and Rh,^{3a,7–16} provide *E* and *Z* isomers depending on the precise nature of the catalysts, substrates, and reaction conditions. In addition, metal-catalyzed isomerization of (*Z*)-vinylsilanes to the most thermodynamically

stable *E* isomer has been observed.^{3a,6a,b,f,8,10} Despite the significant advances made in the last few years for the selective synthesis of the β -(*Z*) and α isomers, few reliable alternatives to Pt(0) catalysts based on phosphine or N-heterocyclic carbene ligands have been envisaged for the synthesis of (*E*)-vinylsilanes (with the exception of some recently reported Au¹⁷ and Co¹⁸ catalysts), whose use is usually hampered by both the high cost and air and moisture sensitivity of the catalysts. Therefore, since highly regio- and stereoselective predictable catalytic systems are limited, even for the more commonly accessible *E* isomer, the development of new catalysts for this transformation is still desirable.

In the case of Rh(I) catalysts, neutral species normally show selectivity toward the formation of β -(*Z*)-vinylsilanes, while cationic complexes provide predominantly β -(*E*)-alkenylsilanes.^{7–9} For example, in the hydrosilylation of alkylalkynes the cationic catalysts formed from [Rh(COD)₂]BF₄ + 2PPh₃ or [Rh(COD)Cl]₂ + 2PPh₃ in polar solvents achieve high regio- and stereoselectivity for β -(*E*)-vinylsilane formation,^{7,10} whereas neutral rhodium complexes such as RhCl(PPh₃)₃ usually afford (*Z*)-alkenylsilanes with moderate to high selectivities.^{6b,11} Moreover, Rh-catalyzed hydrosilylation reactions usually depend on the addition order of the reagents, up to

Received: May 9, 2017

Published: June 16, 2017

the point that some degree of regiocontrol was obtained and a stereodivergent synthesis of the anti-Markovnikov (*Z*)- and (*E*)-alkenylsilanes has been reported using neutral rhodium(I) iodide complexes.¹² In addition, a significant influence of other reaction parameters on selectivity such as concentration,¹¹ solvent,^{10a} and alkyne/silane ratio⁸ have been observed.^{12,13} Another important factor affecting the reaction selectivity is the nature of the silane:¹¹ electron-rich silanes tend to give (*Z*)-olefins with Rh catalysts, while *E* products are obtained with electron-poor hydrosilanes such as (RO)₃SiH. Hence, many *E*-selective rhodium catalysts are limited to the use of R₃SiH silanes that lead to products of low synthetic value.^{2d} Finally, an undesired drawback of Rh catalysts is also the occurrence of competitive processes such as the oligomerization¹⁹ and polymerization of arylalkynes^{9,10b,12b,16a,20} and the formation of alkynylsilanes resulting from the dehydrogenative silylation of the alkynes.^{6b–d,14g}

In the last few years there has been a significant interest in the development of Rh catalysts based on N-heterocyclic carbene (NHC)²¹ ligands for alkyne hydrosilylation.^{13–16} Particularly, focus has been placed, with limited success, on the use of NHC ligands containing hemilabile N-donor groups (Figure 1).^{15,16} For example, initial work by Peris and co-

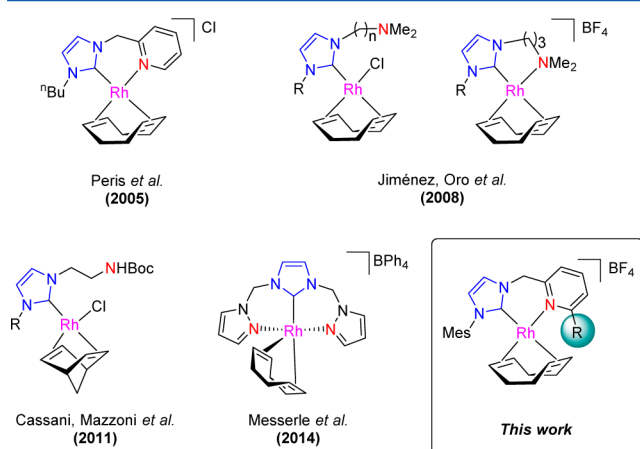


Figure 1. Rh(I) complexes with NHC ligands containing hemilabile N donors for the hydrosilylation of terminal alkynes.

workers has demonstrated the catalytic activity of a picolyl-carbene Rh complex in the addition of HSiMe₂Ph to phenylacetylene.¹⁵ A temperature-dependent *Z* selectivity was observed in this reaction, which was attributed to the isomerization of the initially formed (*Z*)-vinylsilane to the most stable *E* isomer. Neutral and cationic Rh complexes with NHCs containing dimethylamino groups have been reported by Jiménez, Oro, and co-workers.^{16a} Despite the fact that high *Z* selectivity for the reaction of 1-hexyne with HSiMe₂Ph was obtained, the catalysts show an alkyne-dependent selectivity and catalyze the *Z* to *E* isomerization of the resulting vinylsilanes upon prolonged reaction times. In addition, in the reactions of phenylacetylene, extensive polymerization was observed. Similarly, the Cassani and Mazzoni group has reported neutral rhodium(I) BOC-protected amino NHC complexes that are active in the hydrosilylation of terminal alkynes with HSiMe₂Ph.^{16b} Whereas no significant levels of selectivity were observed in the hydrosilylation reaction due to the *Z* to *E* isomerization process, the presence of an hemilabile donor group has been shown to provide a beneficial effect on

the catalyst activity (“anchimeric assistance”).^{16c} Finally, cationic Rh complexes based on tridentate NHC-pyrazole ligands have been shown to catalyze the hydrosilylation of phenylacetylene with triethylsilane, providing modest conversions and selectivities.^{16d}

Herein, we report our studies on the hydrosilylation of acetylenes with a series of new cationic picolyl-NHC-containing Rh complexes that differ in the steric hindrance at the 6-position of the hemilabile pyridine donor. These derivatives provide high catalytic activities and *E* selectivities in the addition of different silanes to a wide range of terminal alkynes. Furthermore, a preliminary mechanistic investigation of the catalytic reactions is also described.

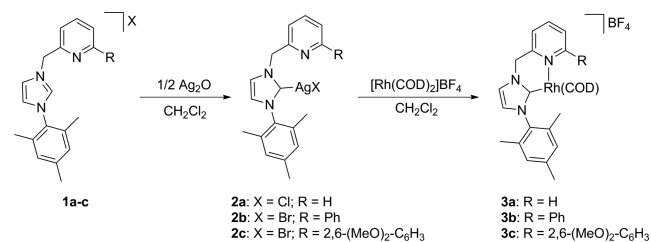
RESULTS AND DISCUSSION

Synthesis and Characterization of Rh Complexes.

Imidazolium salts **1a–c** were easily obtained by alkylation of 1-mesityl-1*H*-imidazole with the corresponding 2-halomethylpyridines, as previously reported.²² NMR spectra of the salts are in agreement with the proposed structures and are consistent with previously reported data for analogous derivatives.

In a subsequent step, the corresponding silver complexes (CN)(AgX) (X = Cl, Br) were prepared to be employed as NHC transfer reagents.²³ Thus, reaction of imidazolium salts **1** with Ag₂O in CH₂Cl₂ at room temperature resulted in the clean formation of silver complexes **2** (Scheme 2),²² as noted by the

Scheme 2. Synthesis of Silver (2) and Rhodium (3) Complexes



disappearance of the imidazolium proton signals at ca. 10 ppm in the ¹H NMR spectra and the appearance of broad signals at ca. 180 ppm in the ¹³C{¹H} NMR experiments due to the C² carbon of the NHC moieties.

In turn, rhodium complexes **3a–c** were conveniently prepared by carbene transfer from the appropriate silver complex **2** to [Rh(COD)₂]₂BF₄ in CH₂Cl₂ at room temperature and were isolated with good yields as yellow-orange crystalline solids after recrystallization from CH₂Cl₂/Et₂O solutions (Scheme 2). Complexes **3** were stable in the solid state under atmospheric conditions. Electrospray mass spectrometry investigation of derivatives **3** produced peaks consistent with the expected molecular ion [M⁺]⁺. Moreover, complexes **3** have been fully characterized by NMR techniques, and all of the complexes were found to show very similar features. For example, in the ¹H NMR spectrum in CD₂Cl₂, the olefinic protons of the COD ligand produce four different signals between 2.3 and 4.8 ppm. In addition, the coordination of the pyridinyl moiety is evidenced from the observation of two doublets for the diastereotopic protons of the CH₂ bridge appearing in the range between 5.7 and 6.5 ppm (²J_{HH} = 14–15 Hz). The ¹³C{¹H} NMR spectra show one doublet signal for the C²(NHC)-Rh carbon at ca. 178 ppm (J_{CRh} = 52 Hz).

To gain further insight into the structure of coordinated picolyl-NHC ligands in complexes **3**, crystals suitable for X-ray diffraction analysis of **3a,c** were obtained by slow diffusion of Et₂O into saturated solutions of CH₂Cl₂ (Figure 2 and Table

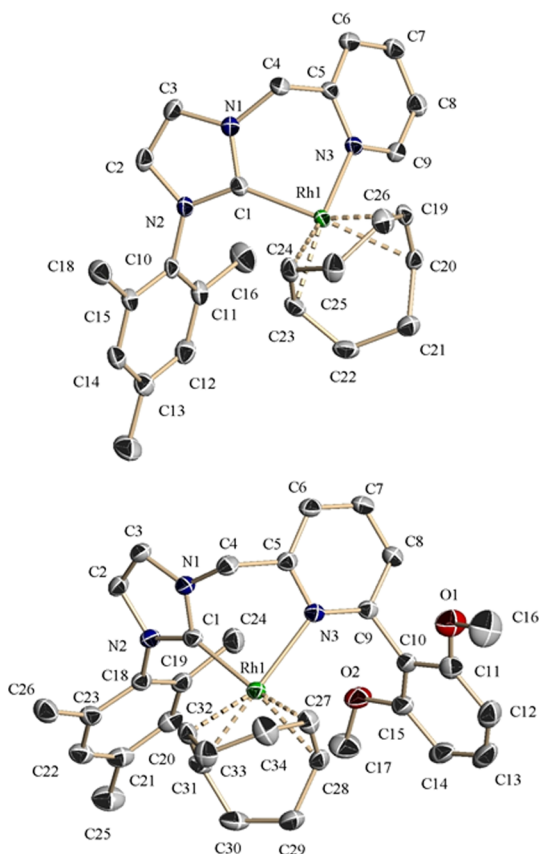


Figure 2. ORTEP drawings at 30% ellipsoid probability of the cationic fragments of complexes **3a** (top) and **3c** (bottom). Hydrogen atoms have been omitted for clarity.

1).^{22a} In these complexes, the rhodium atom displays a square-planar geometry with the pyridine-imidazolynilidene ligand coordinated as a chelate. The bite angle of the picolyl-NHC ligand is ca. 84°. The C²(NHC)–Rh and N–Rh bond lengths are similar to previously found distances,^{22a,24} although a significantly shorter Rh–N distance for **3a** than for **3c** (ca. 0.1 Å) has been found, probably as a consequence of the higher steric encumbrance due to the aryl substituent of the pyridine fragment. The average distances of the C_{COD}–Rh trans to the NHC are longer than those in the cis arrangement ($\Delta d(\text{Rh}-\text{centroid C}=\text{C}) = 0.09 \text{ \AA}$ (**3a**) and 0.13 Å (**3c**)), as expected from the greater trans influence of the carbene donor. Also of interest, the chelate ring adopts a boat conformation that makes the two CH₂ bridge protons nonequivalent, as previously inferred from the solution NMR study.

Dynamic Behavior of Complexes **3** in Solution.

Dynamic hemilabile coordination of heteroditopic ligands has been shown to enhance the catalytic performance by creating transient vacant coordination sites and stabilizing unsaturated catalytic intermediates.²⁵ Since the hemilabile character of the picolyl-NHC ligands can be anticipated due to the presence of a strong σ -donor NHC fragment and a more weakly bound sp²-N function, the solution dynamics of complexes **3a–c** in CD₂Cl₂ and CD₃CN have been studied by ¹H,¹H-EXSY and VT-¹H NMR spectroscopy.

In CD₂Cl₂, the ¹H NMR spectra registered between –10 and 55 °C of complex **3a** show the existence of fluxional behavior. At –10 °C the presence of two doublet signals at 6.01 and 5.65 ppm (²J_{HH} = 14.7 Hz) corresponding to the protons of the methylene backbone is observed. These signals significantly broaden upon heating and finally coalesce at 55 °C. Line-shape analysis of the ¹H NMR spectra gives activation parameter values of $\Delta H^\ddagger = 11.4 \text{ kcal/mol}$ and $\Delta S^\ddagger = -13 \text{ eu}$ (Table 2). In the ¹H,¹H-EXSY spectrum of **3a**, intense cross peaks due to chemical exchange are observed between the signals of the two olefinic protons of the CH=CH fragment trans to the NHC and between the alkene protons trans to the pyridine. However, no exchange signals involving the CH= protons trans to NHC and those trans to the N donor were observed. Alternatively, ¹H NMR spectra of CD₂Cl₂ solutions of complexes **3b,c** do not show significant line broadening up to 55 °C and no exchange cross-peaks are observed in their corresponding ¹H,¹H-EXSY spectra (50 °C), suggesting that the dynamic behavior observed for **3a** in CD₂Cl₂ is absent in the case of **3b,c**. Hence, the fluxional behavior of **3a** can be attributed to the interconversion of the two limiting forms resulting from the inversion of the chelate ring through the C–Rh–N coordination plane (Scheme 3).²⁶ In addition, since solid-state Rh–N distances are significantly longer in **3c** than in **3a**, pyridine decoordination should be easier for the former complex, and consequently the CH₂ bridge flipping in **3a** may occur in CD₂Cl₂ without decoordination of the N-donor fragment.

In contrast, in the presence of coordinating solvents, facile pyridine decoordination can be expected.²⁷ Addition of increasing amounts of MeCN (2–200 equiv) to CD₂Cl₂ solutions of **3b** produces significant broadening of the signals caused by the COD olefinic hydrogens and the CH₂ protons of the picolyl-NHC ligand in the ¹H NMR spectra. Thus, the dynamic process for **3a–c** in CD₃CN has also been studied by VT-¹H NMR spectroscopy. At room temperature, the ¹H NMR spectrum of **3a** is characterized by the presence of a broad signal for the CH₂ bridge and two broad signals for the CH= hydrogens, in agreement with a slow interconversion between the two limiting isomers of the complex (Scheme 3). Line-shape analysis of the ¹H NMR spectra registered in the temperature range between –35 and 50 °C indicates that the energy barrier for the dynamic process in CD₃CN is lower than in CD₂Cl₂ (Table 2). In addition, VT-¹H NMR spectroscopy in CD₃CN of **3b** shows that a similar dynamic behavior is

Table 1. X-ray Diffraction Bond Lengths (Å) and Angles (deg) for **3a,c**

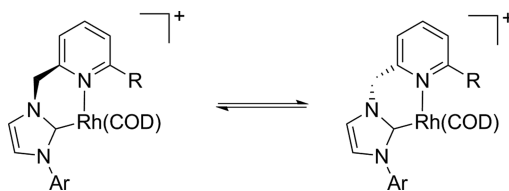
	Rh–C _{NHC}	Rh–N _{Py}	Rh–C=(trans-NHC)	Rh–C=(cis-NHC)	C _{NHC} –Rh–N _{Py}
3a	2.013(3)	2.115(2)	2.187(3) 2.252(3)	2.139(3) 2.131(3)	84.07(10)
3c	2.039(3)	2.213(2)	2.208(3) 2.238(3)	2.107(3) 2.100(3)	84.62(9)

Table 2. Thermodynamic Parameters for the Dynamic Behaviour of Complexes 3a,b^a

	solvent	ΔH^\ddagger (kcal mol ⁻¹)	ΔS^\ddagger (cal mol ⁻¹)	ΔG^\ddagger_{300} (kcal mol ⁻¹)
3a	CD ₂ Cl ₂	11.4(1.6)	-12.8(5.4)	15.3(0.3)
3a	CD ₃ CN	10.1(0.7)	-9.5(2.7)	12.9(0.9)
3b	CD ₃ CN	7.4(1.3)	-28.6(4.5)	16.0(0.1)

^aEstimated standard deviations in parentheses.

Scheme 3. Proposed Dynamic Behavior of Complexes 3



operative for this complex, although the coalescence temperature was not reached at the higher studied temperature (70 °C). Also, the ¹H,¹H-EXSY of 3a,b in CD₃CN only shows pairwise cross peaks for the olefinic protons of the same CH=CH moiety. Therefore, the fluxionality shown by complex 3b, which is not observable in CD₂Cl₂, as well as the lower barrier obtained for 3a in CD₃CN may be ascribed to a fast interconversion between the two limiting isomers facilitated by the lability of the picolyl fragment. Moreover, the negative entropy values found suggest an associative mechanism involving the coordination of CD₃CN.

Alternatively, the dynamic behavior in CD₃CN of the more sterically encumbered complex 3c differs from that of 3a,b, as demonstrated by VT-¹H NMR spectroscopy. The initial AX system observed for the methylene protons of the picolyl-NHC ligand at low temperature is gradually converted to an AB system upon raising the temperature, while the signal from the CH= moieties broadens. Further heating of the sample makes the CH₂ protons equivalent, suggesting that pyridine fragment decoordination occurs leading to a κ^1 -C coordination of the ligand.

Overall, these studies point out the hemilabile character of the pyridine fragment when other donating species (i.e., MeCN) are present and demonstrate the ability of the ligands to exhibit both κ^1 -C and κ^2 -C,N coordination modes.

Catalyst Optimization and Scope. NHC-rhodium catalysts containing N-donor functionalities have provided good levels of activity in the hydrosilylation of alkynes, although low to moderate selectivities have usually been obtained.^{15,16} Thus, the catalytic performance of Rh complexes 3 was examined in the addition of silanes to terminal alkynes. Reaction of ¹²⁹Pr₃SiH with phenylacetylene in CD₂Cl₂ catalyzed by 3a yielded the corresponding β -(*E*)-alkenylsilane accompanied by lower amounts (15%) of the Markovnikov silane addition product (Table 3, entry 1). With the exception of the NHC wingtip, the NHC ligand of complex 3a is structurally similar to that employed by Peris et al., which showed a preference for the formation of the *Z* isomer. This result suggests that the absence of the chloride ligand is beneficial for achieving high selectivity toward the (*E*)-vinylsilane. In addition, the level of stereoselectivity obtained with complex 3a prompted us to examine the catalytic performance of the other complexes. Thus, the reaction with 3b led to a slight increase of the selectivity toward the (*E*)-vinylsilane, while the catalyst derived from 3c completed the reaction with an exquisite regio- and stereoselectivity (entries 2 and 3),²⁸

Table 3. Hydrosilylation of Phenylacetylene with ¹²⁹Pr₃SiH Catalyzed by Complexes 3^a

entry	catalyst	S/C	solvent	yield (%) ^b	<i>E</i> / α
1	3a	200	CD ₂ Cl ₂	100 (4)	85/15
2	3b	200	CD ₂ Cl ₂	100 (4)	89/11
3	3c	200	CH ₂ Cl ₂	100 (2)	99/1
4 ^c	3c	200	THF	99 (2)	99/1
5 ^d	3c	200	MeCN	87 (2)	99/1
6 ^d	3c	200	<i>t</i> -BuOH	97 (2)	99/1
7	3c	200	2Me-THF	81 (2)	98/2
8	3c	1000	CD ₂ Cl ₂	100 (2)	99/1
9	3c	5000	CD ₂ Cl ₂	>99 (24)	99/1

^aReactions were carried out at 60 °C (oil bath), using 0.28 mmol of phenylacetylene and 0.31 mmol of ¹²⁹Pr₃SiH. [phenylacetylene] = 0.6 M. Yield and *E*/ α ratio were determined by ¹H NMR spectroscopy or GC-MS using mesitylene as internal standard. ^bReaction time (in h) in parentheses. ^cOligomerization of phenylacetylene was detected by GC-MS. ^dFormation of poly(phenylacetylene) was observed.

evidencing a significant influence of the size of the hemilabile ligand fragment on the *E*/ α ratio.²⁹ Follow-up of the reaction in CD₂Cl₂ by ¹H NMR spectroscopy showed that the *E*/ α ratio remained practically constant during the reaction course, suggesting that the (*Z*)-vinylsilane is not an intermediate in the formation of the (*E*)-olefin or that there is not a significant accumulation of this isomer. In addition, unlike with previously studied Rh-NHC catalysts,^{16a} formation of other products such as silylacetylenes, resulting from the dehydrogenative silylation of the alkyne, or triphenylbenzenes, formed by trimerization of phenylacetylene, was not observed.

Examination of other solvents showed that there is not a marked influence of the reaction media on the selectivity, although the catalyst activity is somewhat affected (entries 4–7). Trace amounts of acetylene dimerization and cyclo-trimerization were observed by GC-MS analysis when THF was employed as solvent, whereas some polymerization of phenylacetylene was evidenced when MeCN and *t*-BuOH were used. Interestingly, in CD₂Cl₂ the substrate/catalyst ratio could be increased without erosion of the selectivity, providing TOF values of up to 500 h⁻¹ at an S/C ratio of 1000 and 206 h⁻¹ at an S/C ratio of 5000 (entries 8 and 9).

Having determined that complex 3c provides the highest selectivity among the series of Rh complexes, other silanes were tested in the hydrosilylation of phenylacetylene (Table 4). Good activity and selectivity were observed in the addition of PhMe₂SiH and 1,4-bis(dimethylsilyl)benzene (entries 1 and 2). In addition, since vinylalkoxy- and vinylsiloxysilanes are versatile substrates in organic synthesis, particularly in Hiyama cross-coupling reactions,^{1d,e,h,i} the addition of (EtO)₃SiH and (TMSO)₃SiH was examined. In both cases the selectivity was high, although the reaction with the hydrosiloxane was more sluggish. It should be noted that a marked decrease in *E* selectivity for heteroatom-substituted silanes is usually observed with Rh and Pt catalysts.^{2d,3b,8,12}

Table 4. Hydrosilylation of Phenylacetylene Catalyzed by **3c**^a

entry	silane	S/C	yield (%) ^b	<i>E</i> / α
1	PhMe ₂ SiH	2000	100	97/3
2 ^c	1,4-(HSiMe ₂) ₂ C ₆ H ₄	2000	99	97/3
3	(EtO) ₃ SiH	2000	100	96/4
4	(TMSO) ₃ SiH	500	100	99/1

^aReactions were carried out at 60 °C (oil bath) in CD₂Cl₂ using 0.28 mmol of phenylacetylene and 0.31 mmol of silane. [phenylacetylene] = 0.6 M. Yield and *E*/ α ratios were determined by ¹H NMR spectroscopy. ^bReaction time 4 h. ^c0.56 mmol of phenylacetylene was used.

Next, the hydrosilylation of a series of acetylenes was examined using two representative silanes, ⁿPr₃SiH and (EtO)₃SiH (Table 5). Reactions of substituted phenylacetylenes with electron-donating and -withdrawing groups yielded the corresponding (*E*)-vinylsilanes with high selectivity (\geq 96%) (entries 1–8). As previously reported, the regioselectivity obtained with the hydroalkoxysilane is slightly lower than that of ⁿPr₃SiH, although the difference observed is less pronounced than with other catalytic systems.^{2d,3b,8,12}

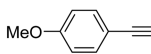

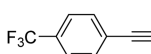
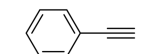
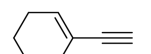
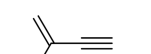
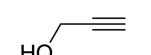
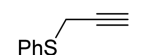
Hex-1-yne was chosen as an example of an alkyl-substituted alkyne, and their reactions with ⁿPr₃SiH and (EtO)₃SiH catalyzed by **3c** proceeded with good conversions and *E* selectivities higher than 96% (Table 5, entries 9 and 10). In addition, it is worth noting that isomerization of the vinylsilane to the corresponding allylsilane, a process previously observed with Pt and Rh catalysts in the hydrosilylation of alkyl-substituted acetylenes, is not observed.^{3a,6b,16a,b} However, the catalyst seems to be sensitive to steric effects, since no reactivity was observed in the reaction of 3,3-dimethylbutyne with ⁿPr₃SiH.

Furthermore, the catalytic system is compatible with a number of functional groups. For example, hydrosilylation of enynes, with both terminal and internal C=C bonds, occurs chemoselectively at the triple C–C bond (Table 5, entries 11–14). In addition, the hydrosilylation of heteroatom-functionalized alkynes was examined. Hydrosilylation addition to a propargylic alcohol occurs at the triple bond with high *E* selectivity, while no silylation of the oxygen atom was observed (entries 15 and 16).³⁰ Finally, the presence of potentially coordinating sulfur atoms did not interfere with the hydrosilylation, although a sluggish reaction was observed with ⁿPr₃SiH (entries 17 and 18).

Mechanistic Considerations. The commonly accepted steps for the hydrosilylation of alkynes are based on the Chalk–Harrod mechanism for alkene hydrosilylation,^{2d,31} which involves the oxidative addition of the silane Si–H bond to the metal, migratory insertion of the coordinated alkyne into the M–H fragment, and reductive elimination of the vinyl and silyl ligands. For some catalytic systems, however, a modified Chalk–Harrod mechanism has been proposed to explain the formation of the *Z* derivatives and dehydrogenative silylation products.^{2d} In this alternative mechanism, alkyne insertion takes place into the Rh–Si bond, which might be followed by *cis*/*trans* isomerization of the resulting vinyl complex through the involvement of metallacyclopentene^{6a,b} or zwitterionic carbene¹¹ species before the reductive elimination step.

To shed light on the mechanism of the reactions catalyzed by complexes **3**, the hydrosilylation of phenylacetylene with ⁿPr₃SiH catalyzed by 20 mol % of complex **3b** in CD₂Cl₂ was

Table 5. Hydrosilylation of Acetylenes with ⁿPr₃SiH and (EtO)₃SiH Catalyzed by **3c**^a

Entry	Alkyne	Silane	S/C	Yield (%) ^b	<i>E</i> / α ratio
1		ⁿ Pr ₃ SiH	500	100 (4 h)	>99/-
2		(EtO) ₃ SiH	500	100 (4 h)	96/4
3		ⁿ Pr ₃ SiH	500	93 (4 h)	>99/ ^c
4		(EtO) ₃ SiH	500	94 (4 h)	98/2
5		ⁿ Pr ₃ SiH	500	98 (4 h)	98/2
6		(EtO) ₃ SiH	500	98 (4 h)	97/3
7		ⁿ Pr ₃ SiH	500	87 (8 h)	98/2
8		(EtO) ₃ SiH	500	100 (4 h)	97/3
9	1-Hexyne	ⁿ Pr ₃ SiH	200	97 (4 h)	99/1
10		(EtO) ₃ SiH	500	91 (4 h)	96/4
11		ⁿ Pr ₃ SiH	500	100 (4 h)	99/1
12		(EtO) ₃ SiH	500	100 (4 h)	96/4
13		ⁿ Pr ₃ SiH	500	100 (4 h)	99/1
14		(EtO) ₃ SiH	500	100 (4 h)	^d
15 ^e		ⁿ Pr ₃ SiH	5000	100 (4 h)	>99/-
16		(EtO) ₃ SiH	500	95 (4 h)	83/17
17		ⁿ Pr ₃ SiH	500	26 (4 h) ^f	99/1
18		(EtO) ₃ SiH	500	100 (4 h)	95/5

^aReactions were carried out at 60 °C (oil bath) in CD₂Cl₂ using 0.28 mmol of acetylene and 0.31 mmol of ⁿPr₃SiH or (EtO)₃SiH. [alkyne] = 0.6 M. Yield and *E*/ α ratios were determined by ¹H NMR spectroscopy. ^bReaction time in parentheses. ^cMinor amounts, less than 2%, of the β -(*Z*)-vinylsilane were observed. ^d β -(*E*)/ β -(*Z*)/ α = 91/2/7. ^e[alkyne] = 0.3 M. ^fA longer reaction time (72 h) did not increase conversion.

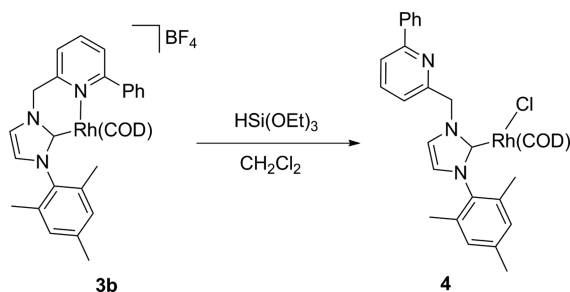
followed up by ¹H NMR spectroscopy. Interestingly, no intermediates, to the detection limit of ¹H NMR spectroscopy, were observed, since the signals corresponding to the Rh precursor appeared unchanged. This observation suggests that

the catalyst is formed in a very low concentration, below the NMR detection limit, from the catalyst precursor **3b**.

Next, the reactivity of the Rh precursors with the coupling partners was studied individually. Addition of a slight excess of phenylacetylene (5 equiv) to a solution of **3b** in CD_2Cl_2 or CD_3CN produces no changes, to the detection limit of the technique, in the signals of the ^1H NMR spectrum of the Rh complex, whereas the resonances of phenylacetylene gradually disappear and new broad signals are observed in the aromatic region. These changes are accompanied by the formation of an insoluble red solid resulting from alkyne polymerization.³²

On the other hand, prolonged heating of a solution of **3b** and triethoxysilane (15 equiv) in CD_2Cl_2 yields complex **4** (Scheme 4). A similar reaction outcome is observed when tripropylsilane

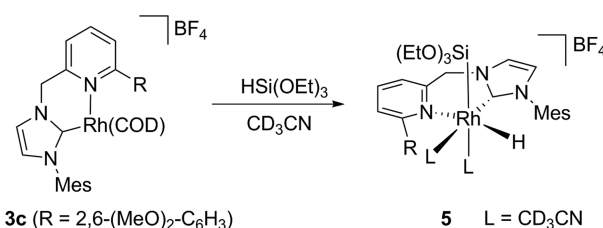
Scheme 4. Reaction of Complex **3b** with $\text{HSi}(\text{OEt})_3$ in CH_2Cl_2



is employed; however, the reactions are accompanied by abundant formation of a black metallic precipitate. In the ^1H NMR spectrum of **4** registered in CD_2Cl_2 , four different signals between 3.0 and 4.8 ppm attributable to the olefinic protons of the COD ligand are observed, as well as two doublets for the diastereotopic protons of the CH_2 bridge appearing at 5.74 and 6.77 ppm ($^2J_{\text{HH}} = 15.7$ Hz) that reflect a hindered rotation of the NHC ligand around the $\text{C}^2(\text{NHC})\text{-Rh}$ bond. The $^{13}\text{C}\{^1\text{H}\}$ NMR spectrum shows one doublet signal for the $\text{C}^2(\text{NHC})$ carbon at δ 184 ppm ($J_{\text{CRh}} = 52$ Hz) and two pairs of doublets for the olefinic carbons, one in the range 68–69 ppm ($J_{\text{CRh}} = 14$ Hz) and other at 96–98 ppm ($J_{\text{CRh}} = 7$ Hz). Electrospray mass spectrometry investigation of **4** produced peaks consistent with the expected ion $[\text{M} - \text{Cl}]^+$. The structural assignment for complex **4**, having a coordinated NHC fragment and a dangling pyridyl moiety, is further supported by comparison of their NMR data with those reported for similar complexes by Liu and co-workers.^{22a} Testing of complex **4** in the hydrosilylation of phenylacetylene with $^n\text{Pr}_3\text{SiH}$ ($S/C = 100$, 60°C , CD_2Cl_2) resulted in a significantly different catalytic activity and product distribution in comparison to that provided by **3b**, since the product ratio $E/Z/\alpha/\text{styrene/silylacetylene} = 84/3/5/3/5$ was obtained (81% conversion, 24 h), in line with the negligible formation of **4** from **3b** under catalytic conditions and making evident the beneficial effect of using a catalyst precursor with a noncoordinating counteranion.

Interestingly, alternative heating of **3c** in CD_3CN with an excess of triethoxysilane shows the formation of a new species that has been assigned to the silyl hydrido Rh complex **5**, resulting from the formal activation of the silane Si-H bond (Scheme 5). GC-MS analysis of the reaction mixture shows the formation of cyclooctene as well as $\text{Si}(\text{OEt})_4$ and minor amounts of other unidentified silicon species. The ^1H NMR spectrum of the silylrhodium hydride **5** shows the appearance

Scheme 5. Reaction of Complex **3c** with $\text{HSi}(\text{OEt})_3$ in CD_3CN

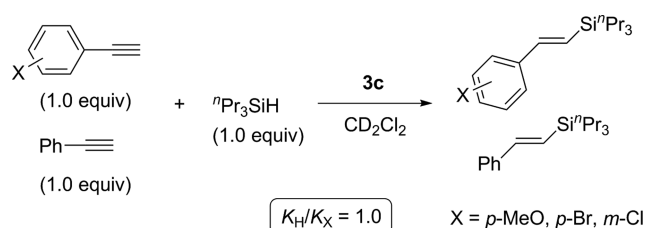


of a doublet at -17.46 ppm ($^1J_{\text{HRh}} = 30.8$ Hz) attributable to the Rh-H functionality and two doublets at 5.36 and 6.00 ppm ($^2J_{\text{HH}} = 14.8$ Hz) for the diastereotopic protons of the CH_2 linker. The signals corresponding to the silyl ligand $\text{Si}(\text{OCH}_2\text{CH}_3)_3$ appear at 0.99 and 3.60 ppm as a triplet and a quartet ($^3J_{\text{HH}} = 7.0$ Hz), respectively. The $^{13}\text{C}\{^1\text{H}\}$ NMR spectrum shows the signal corresponding to the carbenic carbon at 173.6 ppm as a doublet ($^1J_{\text{CRh}} = 54$ Hz). In addition, the 2D NMR heteronuclear correlation $^1\text{H},^{29}\text{Si}$ HMBC exhibits a cross-peak doublet signal at -34.3 ppm ($^1J_{\text{SiRh}} = 62$ Hz) between the hydride and the silicon atom of **5**. Finally, an intense cross peak was observed in the $^1\text{H},^1\text{H}$ NOESY experiment between the Rh-H and $\text{SiOCH}_2\text{CH}_3$ hydrogens, suggesting a *cis* arrangement for the hydrido and silyl ligands. Analysis of **5** by ESI-MS provides a peak at m/z 680 attributable to the ion $[\text{M} - 2\text{MeCN} - \text{BF}_4]^+$. In support of the proposed Ir complex has been previously reported by Peris and co-workers.^{6d} Finally, in order to examine the catalytic performance of **5**, a 6-fold equimolar amount of triethoxysilane and phenylacetylene was added to a solution in CD_2Cl_2 of **5**, yielding the hydrosilylation product with a E/α ratio of 96/4 along with the starting complex and therefore suggesting that **5** is involved in the catalytic cycle.

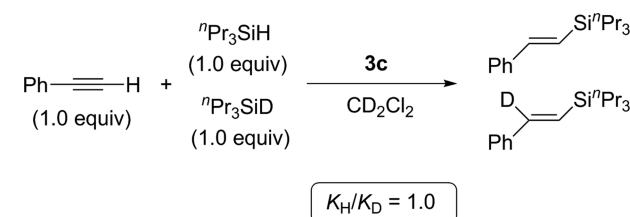
Next, we studied the influence of electronic effects on the rate of hydrosilane addition to substituted phenylacetylenes. Preliminary experiments showed significantly faster reactions for arylalkynes containing electron-donating groups than for alkynes having electron-withdrawing substituents. However, this observation might be caused by intrinsically different catalytic cycle rates or be due to differences in precatalyst activation if the alkyne plays a role in the formation of the active species: for example, by promoting the decoordination of the pyridine fragment of the picolyl-NHC ligand in analogy to the observed influence of MeCN on the dynamic properties of complexes **3** (see above). In order to eliminate the influence of the catalyst formation step on the reaction rate, a series of competition reactions involving the hydrosilylation of equimolar amounts of phenylacetylene and $\text{X-C}_6\text{H}_4\text{C}\equiv\text{CH}$ ($\text{X} = p\text{-MeO}$, $p\text{-Br}$, $m\text{-Cl}$) with $^n\text{Pr}_3\text{SiH}$ were investigated (Scheme 6). In all of the experiments, both acetylenes reacted at the same rate, demonstrating that the catalytic reactions are insensitive to the electronic nature of the alkyne.

The study of kinetic isotope effects (KIEs) provides a straightforward method to obtain relevant mechanistic information and support the proposal of reaction mechanisms.³³ Thus, catalytic reactions with selectively deuterated substrates were performed. From the reaction of phenylacetylene (1.0 equiv) with $^n\text{Pr}_3\text{SiH}$ (1.0 equiv) and $^n\text{Pr}_3\text{SiD}$ (1.0 equiv) (Scheme 7), $K_{\text{H}}/K_{\text{D}} = 1.0$ was found, suggesting that oxidative addition of the hydrosilane is not involved in the rate-determining step. Alternatively, for the reaction of $\text{C}_6\text{H}_5\text{C}\equiv$

Scheme 6. Determination of Electronic Effects on the Hydrosilylation Rates

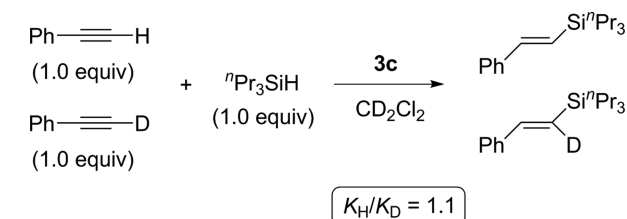


Scheme 7. Determination of KIE using Deuterated Silane



CH (1.0 equiv) and $C_6H_5C\equiv CD$ (1.0 equiv) with nPr_3SiH (1.0 equiv) (Scheme 8), the secondary kinetic isotope effect

Scheme 8. Determination of KIE using Deuterated Alkyne



$K_H/K_D = 1.1$ was determined. In addition, from the study of the geometry of the obtained deuterated products in these experiments, syn addition of the silane to the alkyne was evidenced.

Although further mechanistic studies are required, the assumption of Chalk–Harrod mechanisms for the hydrosilylation of alkynes catalyzed by Rh complexes 3 seems

plausible on the basis of the above experimental data and literature precedents (Figure 3). After initial formation of the hydrido-silyl Rh species A (i.e., 5), alkyne coordination should take place to yield B. From this intermediate, two different outcomes involving the migratory insertion of the alkyne into the Rh–H bond are possible, depending on the orientation of the insertion step (1,2 or 2,1). An alkyne 1,2-insertion would lead to vinyl Rh species $C^H(E)$, which after reductive elimination and activation of a new silane molecule would regenerate A and afford the major (*E*)-vinylsilane derivative. Alternative 2,1-insertion into the Rh–H bond would produce $C^H(\alpha)$, which ultimately would yield the α -vinylsilane. Similar pathways involving intermediates $C^{Si}(E)$ and $C^{Si}(\alpha)$ can be regarded if, instead of the migratory insertion of the alkyne into the Rh–H bond, the silyl group is delivered to the coordinated alkyne (modified Chalk–Harrod mechanism). Since the reaction regioselectivity is given by the migratory insertion step, analysis of intermediates C can provide clues about the operative mechanism. If insertion into the Rh–H bond is considered, formation of intermediate $C^H(\alpha)$ should be disfavored on the basis of steric grounds, and an increase in the steric crowding of the pyridine fragment of the picolyl-NHC ligand would provide higher anti-Markovnikov selectivity, as observed in the reactions catalyzed by complexes 3 (Table 3). Alternatively, if silyl delivery to the coordinated alkyne takes place, steric hindrance should disfavor the formation of $C^{Si}(E)$ over $C^{Si}(\alpha)$. Hence, we hypothesized that a standard Chalk–Harrod mechanism is operative with complexes 3. However, since formation of minor amounts of *Z* isomers has been observed in some reactions (Table 5, entries 3 and 14), which may be explained by the partial isomerization of $C^{Si}(E)$ to $C^{Si}(Z)$, the occurrence of a modified Chalk–Harrod mechanism cannot be completely excluded.

CONCLUSIONS

A series of Rh(I) complexes 3 containing picolyl-NHC ligands differing in the steric crowding at the 6-position of the pyridine moiety has been synthesized, and the hemilabile nature of the N-donor fragment has been demonstrated by NMR spectroscopy. Complexes 3 activate the H–Si bonds of silanes to yield silyl hydrido Rh species, such as 5, that are efficient catalysts in

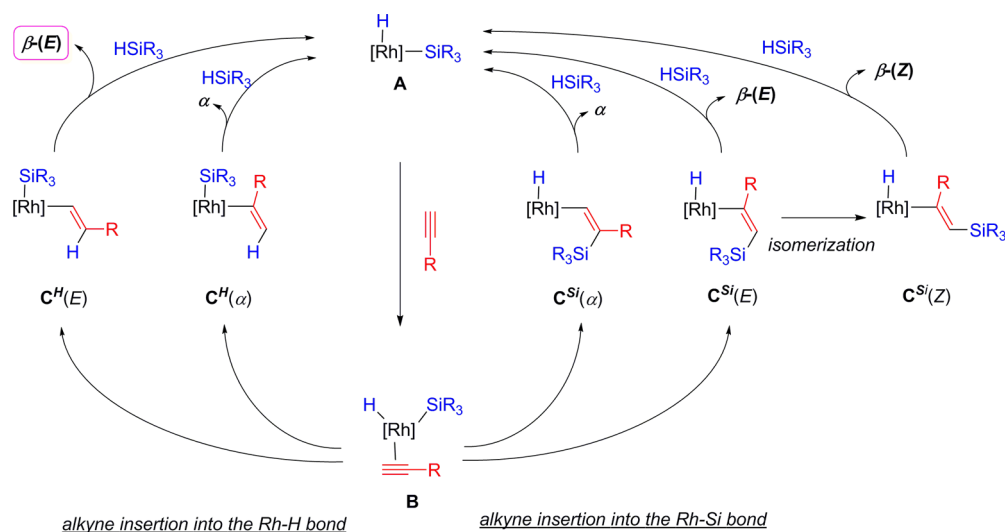


Figure 3. Proposed pathways for the standard and modified Chalk–Harrod mechanisms for alkyne hydrosilylation catalyzed by 3.

the *E*-selective hydrosilylation of terminal alkynes. Although the catalytic activities provided by these catalysts are still far from that of the very active Pt(0) species, to the best of our knowledge, this catalytic system is only surpassed in terms of activity by only two other rhodium(I) *E*-selective catalysts,^{10b,12b} while the high selectivity toward the formation of (*E*)-vinylsilanes and wide alkyne and silane scope make these alkyne hydrosilylation catalysts of practical interest. In addition, this study highlights the importance of ligand design for the development of selective Rh catalysts for the hydrosilylation of alkynes, since a significant influence of the steric hindrance of the hemilabile ligand fragment on the *E*/ α ratio has been evidenced.²⁹

EXPERIMENTAL SECTION

General Procedures. All reactions and manipulations were performed under nitrogen or argon, either in a Braun Labmaster 100 glovebox or using standard Schlenk-type techniques. All solvents were dried over appropriate drying agents and distilled under nitrogen. NMR spectra were obtained on Bruker DPX-300, DRX-400, or DRX-500 spectrometers. $^{13}\text{C}\{^1\text{H}\}$ and ^1H shifts were referenced to the residual signals of deuterated solvents. All data are reported in ppm downfield from Me_4Si . ESI-MS experiments were carried out in a Bruker 6000 apparatus by the Mass Spectrometry Service of the Instituto de Investigaciones Químicas. Elemental analyses were run by the Analytical Service of the Instituto de Investigaciones Químicas in a Leco CHNS-932 elemental analyzer.

Synthesis of Rh Complexes 3. A solution of the corresponding silver complex **2** (0.24 mmol) and $[\text{Rh}(\text{COD})_2]\text{BF}_4$ (0.094 g, 0.24 mmol) in CH_2Cl_2 (8 mL) was stirred for 4 h. The mixture was filtered through a short pad of Celite, and the solution was brought to dryness. The resulting solid was washed with Et_2O (3×10 mL) and recrystallized from a $\text{CH}_2\text{Cl}_2/\text{Et}_2\text{O}$ mixture.

Complex 3a. Yellow-orange solid (63%). Anal. Calcd for $\text{C}_{26}\text{H}_{31}\text{BF}_4\text{N}_3\text{Rh}$ (%): C 54.29; H 5.43; N 7.30. Found: C 54.29; H 5.50; N 7.09. MS (ESI, $\text{CH}_2\text{Cl}_2/\text{MeOH}$): m/z 488 ($[\text{M}^+]^+$, 100). ^1H NMR (CD_2Cl_2 , 400 MHz): δ 1.75–2.48 (m, 8H, 8 *CHH* COD), 2.02 (s, 6H, 2 CH_3), 2.38 (s, 3H, CH_3), 3.30 (br, 1H, $\text{CH}=\text{COD}$), 4.25 (br, 1H, $\text{CH}=\text{COD}$), 4.45 (br, 1H, $\text{CH}=\text{COD}$), 4.51 (br, 1H, $\text{CH}=\text{COD}$), 5.72 (br d, $^2J_{\text{HH}} = 13.5$ Hz, 1H, *py*-*CHH*), 6.05 (br d, $^2J_{\text{HH}} = 13.8$ Hz, 1H, *py*-*CHH*), 6.81 (d, $^3J_{\text{HH}} = 1.8$ Hz, 1H, H arom), 7.01 (br s, 1H, H arom), 7.09 (br s, 1H, H arom), 7.43 (ddd, $^3J_{\text{HH}} = 5.8$ Hz, $^3J_{\text{HH}} = 5.8$ Hz, $^4J_{\text{HH}} = 3.1$ Hz, 1H, H arom), 7.59 (d, $^3J_{\text{HH}} = 1.8$ Hz, 1H, H arom), 7.95 (m, 2H, 2 H arom), 8.35 (d, $^3J_{\text{HH}} = 5.4$ Hz, 1H, H arom). $^{13}\text{C}\{^1\text{H}\}$ NMR (CD_2Cl_2 , 101 MHz): δ 17.9 (br s, CH_3), 19.1 (br s, CH_3), 21.2 (CH_3), 28.2 (br s, CH_2 COD), 30.4 (br s, CH_2 COD), 31.4 (br s, CH_2 COD), 33.3 (br s, CH_2 COD), 56.2 (*py*- CH_2), 77.0 (br m, $\text{CH}=\text{COD}$), 79.1 (br m, $\text{CH}=\text{COD}$), 97.0 (br m, $\text{CH}=\text{COD}$), 98.9 (br m, $\text{CH}=\text{COD}$), 122.7 (CH arom), 123.5 (CH arom), 125.8 (CH arom), 126.2 (CH arom), 129.0 (C_q arom), 129.5 (br s, 2 CH arom), 134.9 (br s, C_q arom), 135.7 (br s, C_q arom), 140.0 (C_q arom), 140.1 (CH arom), 151.3 (CH arom), 154.5 (C_q arom), 177.7 (d, $J_{\text{CRh}} = 52$ Hz, C-2 NHC).

Complex 3b. Yellow-orange solid (59%). Anal. Calcd for $\text{C}_{32}\text{H}_{35}\text{BF}_4\text{N}_3\text{Rh}$: C, 59.01; H, 5.42; N, 6.45. Found: C, 59.19; H, 5.57; N, 6.41. MS (ESI, $\text{CH}_2\text{Cl}_2/\text{MeOH}$): m/z 564 ($[\text{M}^+]^+$, 100). ^1H NMR (CD_2Cl_2 , 400 MHz): δ 1.23 (m, 2H, 2 *CHH* COD), 1.56 (m, 1H, *CHH* COD), 1.89 (s, 3H, CH_3), 2.05 (s, 3H, CH_3), 2.07 (m, 4H, 4 *CHH* COD), 2.47 (s, 3H, CH_3), 2.49 (m, 2H, *CHH* COD + $\text{CH}=\text{COD}$), 3.70 (m, 1H, $\text{CH}=\text{COD}$), 4.03 (m, 1H, $\text{CH}=\text{COD}$), 4.29 (m, 1H, $\text{CH}=\text{COD}$), 5.99 (d, $^2J_{\text{HH}} = 14.8$ Hz, 1H, *py*-*CHH*), 6.48 (d, $^2J_{\text{HH}} = 14.8$ Hz, 1H, *py*-*CHH*), 6.88 (s, 1H, H arom), 7.08 (s, 1H, H arom), 7.19 (s, 1H, H arom), 7.63 (dd, $^3J_{\text{HH}} = 7.5$ Hz, $^3J_{\text{HH}} = 7.5$ Hz, 2H, 2 H arom), 7.71 (t, $^3J_{\text{HH}} = 7.0$ Hz, 1H, H arom), 7.76 (d, $^3J_{\text{HH}} = 7.0$ Hz, 1H, H arom), 7.77 (s, 1H, H arom), 8.03 (d, $^3J_{\text{HH}} = 7.2$ Hz, 1H, H arom), 8.07 (dd, $^3J_{\text{HH}} = 7.5$ Hz, $^3J_{\text{HH}} = 7.5$ Hz, 1H, H arom), 8.32 (d, $^3J_{\text{HH}} = 7.4$ Hz, 2H, 2 H arom). $^{13}\text{C}\{^1\text{H}\}$ NMR (CD_2Cl_2 , 101 MHz): δ 17.8 (CH_3), 17.9 (CH_3), 21.3 (CH_3), 25.9 (CH_2 COD), 29.6

(CH_2 COD), 31.8 (CH_2 COD), 34.9 (CH_2 COD), 56.8 (*py*- CH_2), 73.9 (d, $J_{\text{CRh}} = 12$ Hz, $\text{CH}=\text{COD}$), 75.7 (d, $J_{\text{CRh}} = 14$ Hz, $\text{CH}=\text{COD}$), 92.8 (d, $J_{\text{CRh}} = 7$ Hz, $\text{CH}=\text{COD}$), 100.7 (d, $J_{\text{CRh}} = 8$ Hz, $\text{CH}=\text{COD}$), 123.4 (CH arom), 123.7 (CH arom), 124.3 (CH arom), 125.0 (CH arom), 127.0 (2 CH arom), 128.9 (CH arom), 129.5 (3 CH arom), 131.6 (CH arom), 135.3 (C_q arom), 135.4 (C_q arom), 135.8 (C_q arom), 139.4 (C_q arom), 140.0 (CH arom), 140.3 (C_q arom), 155.1 (C_q arom), 161.1 (C_q arom), 177.0 (d, $J_{\text{CRh}} = 52$ Hz, C-2 NHC).

Complex 3c. Yellow-orange solid (63%). Anal. Calcd for $\text{C}_{34}\text{H}_{39}\text{BF}_4\text{N}_3\text{O}_2\text{Rh}$: C, 57.40; H, 5.53; N, 5.91. Found: C, 57.25; H, 5.53; N, 5.85. MS (ESI, $\text{CH}_2\text{Cl}_2/\text{MeOH}$): m/z 624 ($[\text{M}^+]^+$, 100). ^1H NMR (CD_2Cl_2 , 400 MHz): δ 1.31 (m, 1H, *CHH* COD), 1.45 (m, 2H, 2 *CHH* COD), 1.91 (m, 4H, 4 *CHH* COD), 1.92 (s, 3H, CH_3), 2.05 (s, 3H, CH_3), 2.35 (s, 3H, CH_3), 2.37 (m, 1H, *CHH* COD), 3.16 (m, 1H, $\text{CH}=\text{COD}$), 3.34 (m, 1H, $\text{CH}=\text{COD}$), 3.62 (s, 3H, OCH_3), 3.63 (s, 3H, OCH_3), 3.77 (m, 1H, $\text{CH}=\text{COD}$), 4.82 (m, 1H, $\text{CH}=\text{COD}$), 5.78 (d, $^2J_{\text{HH}} = 14.3$ Hz, 1H, *py*-*CHH*), 6.42 (d, $^2J_{\text{HH}} = 14.4$ Hz, 1H, *py*-*CHH*), 6.58 (d, $^3J_{\text{HH}} = 8.3$ Hz, 1H, H arom), 6.75 (d, $^3J_{\text{HH}} = 8.7$ Hz, 1H, H arom), 6.76 (s, 1H, H arom), 6.96 (s, 1H, H arom), 7.03 (s, 1H, H arom), 7.25 (d, $^3J_{\text{HH}} = 7.5$ Hz, 1H, H arom), 7.44 (dd, $^3J_{\text{HH}} = 8.3$ Hz, $^3J_{\text{HH}} = 8.3$ Hz, 1H, H arom), 7.64 (s, 1H, H arom), 7.86 (d, $^3J_{\text{HH}} = 7.5$ Hz, 1H, H arom), 7.91 (dd, $^3J_{\text{HH}} = 7.5$ Hz, $^3J_{\text{HH}} = 7.5$ Hz, 1H, H arom). $^{13}\text{C}\{^1\text{H}\}$ NMR (CD_2Cl_2 , 126 MHz): δ 18.0 (CH_3), 18.9 (CH_3), 21.1 (CH_3), 26.9 (CH_2 COD), 30.1 (CH_2 COD), 31.1 (CH_2 COD), 34.7 (CH_2 COD), 55.8 (*py*- CH_2), 57.0 (OCH_3), 57.1 (OCH_3), 69.3 (d, $J_{\text{CRh}} = 13$ Hz, $\text{CH}=\text{COD}$), 73.7 (d, $J_{\text{CRh}} = 15$ Hz, $\text{CH}=\text{COD}$), 96.8 (d, $J_{\text{CRh}} = 7$ Hz, $\text{CH}=\text{COD}$), 99.1 (d, $J_{\text{CRh}} = 7$ Hz, $\text{CH}=\text{COD}$), 103.9 (CH arom), 105.0 (CH arom), 117.6 (C_q arom), 122.2 (CH arom), 124.2 (2 CH arom), 129.4 (CH arom), 129.5 (CH arom), 129.6 (CH arom), 132.0 (CH arom), 135.0 (C_q arom), 135.6 (C_q arom), 135.8 (C_q arom), 139.2 (CH arom), 139.7 (C_q arom), 154.8 (C_q arom), 158.6 (C_q arom), 158.7 (C_q arom), 159.4 (C_q arom), 177.8 (d, $J_{\text{CRh}} = 52$ Hz, C-2 NHC).

Procedure for the Generation of Complex 5. A solution of complex **3c** (0.025 g, 0.03 mmol) and $\text{HSi}(\text{OEt})_3$ (32 μL , 0.17 mmol) in CD_3CN (0.7 mL) was heated at 60 °C for 16 h. Volatiles were removed under vacuum, and the residue was dissolved in CD_3CN and analyzed by NMR spectroscopy. Further attempts to purify complex **5** only produced significant decomposition. Signal assignments in the ^1H and $^{13}\text{C}\{^1\text{H}\}$ NMR spectra were made with the assistance of 2D NMR spectroscopy, including ^1H , ^1H -COSY, ^1H , ^1H -NOESY, ^1H , $^{13}\text{C}\{^1\text{H}\}$ -HMQC, and ^1H , $^{13}\text{C}\{^1\text{H}\}$ -HMBC experiments.

^1H NMR (CD_3CN , 400 MHz): δ -17.46 (d, $^1J_{\text{Hrh}} = 30.8$ Hz, 1H, RhH), 0.99 (t, $^3J_{\text{HH}} = 7.0$ Hz, 9H, 3 $\text{SiOCH}_2\text{CH}_3$), 1.70 (s, 3H, CH_3), 2.25 (s, 3H, CH_3), 2.37 (s, 3H, CH_3), 3.60 (q, $^3J_{\text{HH}} = 7.0$ Hz, 6H, 3 SiOCH_2), 3.84 (overlapped, 6H, 2 OCH_3), 5.36 (d, $^2J_{\text{HH}} = 14.8$ Hz, 1H, *py*-*CHH*), 6.00 (d, $^2J_{\text{HH}} = 14.8$ Hz, 1H, *py*-*CHH*), 6.80 (br d, $^3J_{\text{HH}} = 8.8$ Hz, 2H, 2 H arom), 7.00 (d, $^3J_{\text{HH}} = 1.9$ Hz, 1H, H arom), 7.02 (s, 1H, H arom), 7.11 (s, 1H, H arom), 7.44 (t, $^3J_{\text{HH}} = 8.8$ Hz, 1H, H arom), 7.46 (d, $^3J_{\text{HH}} = 1.9$ Hz, 1H, H arom), 7.50 (d, $^3J_{\text{HH}} = 7.8$ Hz, 1H, H arom), 7.70 (dd, $^3J_{\text{HH}} = 7.7$ Hz, $^4J_{\text{HH}} = 1.2$ Hz, 1H, H arom), 8.03 (dd, $^3J_{\text{HH}} = 7.7$ Hz, $^3J_{\text{HH}} = 7.7$ Hz, 1H, H arom). ^1H , ^{29}Si -HMQC (CD_3CN): δ -34.3 ppm (d, $J_{\text{SiRh}} = 62$ Hz). $^{13}\text{C}\{^1\text{H}\}$ NMR (CD_3CN , 101 MHz): δ 18.0 (CH_3), 18.3 (3 $\text{SiOCH}_2\text{CH}_3$), 21.1 (CH_3), 56.4 (*py*- CH_2), 58.6 (3 $\text{SiOCH}_2\text{CH}_3$), 106.1 (CH arom), 123.0 (CH arom), 124.0 (CH arom), 124.8 (CH arom), 129.7 (2 CH arom), 130.3 (2 CH arom), 132.5 (CH arom), 136.7 (C_q arom), 137.2 (C_q arom), 137.3 (C_q arom), 139.9 (CH arom), 140.2 (C_q arom), 155.6 (C_q arom), 157.5 (C_q arom), 159.4 (2 C_q arom), 173.6 (d, $J_{\text{CRh}} = 54$ Hz, C-2 NHC). Signals corresponding to one CH_3 from the mesityl fragment, the two OCH_3 , and one quaternary aromatic carbon could not be unambiguously assigned. MS (ESI, MeCN): m/z 680 ($[\text{M} - 2\text{MeCN} - \text{BF}_4]^+$, 100). Fragmentation of ion m/z 680: m/z 516 ($[\text{M} - 2\text{MeCN} - \text{BF}_4 - \text{HSi}(\text{OEt})_3]^+$, 100).

Representative Procedure for Catalytic Hydrosilylation Reactions. In a glovebox, an NMR tube was charged with a solution of complex **3c** (0.4 mg, 0.56 μmol), phenylacetylene (31 μL , 0.28 mmol), and tri-*n*-propylsilane (57 μL , 0.31 mmol) in CD_2Cl_2 (0.5 mL). The reaction mixture was heated to 60 °C (oil bath) for 4 h.

Conversion was determined by ^1H NMR spectroscopy or GC-MS using mesitylene as internal standard, while the E/α ratio was obtained by ^1H NMR spectroscopy.

■ ASSOCIATED CONTENT

Supporting Information

The Supporting Information is available free of charge on the ACS Publications website at DOI: 10.1021/acs.organomet.7b00361.

Synthetic procedures and analytical data for derivatives 1, 2, and 4, NMR spectra, VT- ^1H NMR spectra of 3, analytical data of hydrosilylation products, competition experiments, and X-ray diffraction details (PDF)

Accession Codes

CCDC 1539440–1539441 contain the supplementary crystallographic data for this paper. These data can be obtained free of charge via www.ccdc.cam.ac.uk/data_request/cif, or by emailing data_request@ccdc.cam.ac.uk, or by contacting The Cambridge Crystallographic Data Centre, 12 Union Road, Cambridge CB2 1EZ, UK; fax: +44 1223 336033.

■ AUTHOR INFORMATION

Corresponding Authors

*E-mail for V.S.: salazar@uaeh.edu.mx.

*E-mail for A.S.: andres.suarez@iiq.csic.es.

ORCID

Andrés Suárez: 0000-0002-0487-611X

Notes

The authors declare no competing financial interest.

■ ACKNOWLEDGMENTS

Financial support (FEDER contribution) from the Spanish MINECO (CTQ2013-45011-P, CTQ2016-80814-R, and CTQ2016-81797-REDC) is gratefully acknowledged. P.L. thanks the Spanish MINECO for a Juan de la Cierva contract. Prof. Ernesto Carmona (IIQ) is thanked for a generous loan of catalyst for silane deuteration.

■ REFERENCES

- (1) (a) Langkopf, E.; Schinzer, D. *Chem. Rev.* **1995**, *95*, 1375–1408. (b) Fleming, I.; Dunogues, J.; Smithers, R. *Org. React.* **1989**, *37*, 57–575. (c) Fleming, I.; Barbero, A.; Walter, D. *Chem. Rev.* **1997**, *97*, 2063–2192. (d) Denmark, S. E.; Ober, M. H. *Aldrichimica Acta* **2003**, *36*, 75–85. (e) Denmark, S. E.; Sweis, R. F. *Acc. Chem. Res.* **2002**, *35*, 835–846. (f) Blumenkopf, T. A.; Overman, L. E. *Chem. Rev.* **1986**, *86*, 857–873. (g) Jones, G. R.; Landais, Y. *Tetrahedron* **1996**, *52*, 7599–7662. (h) Hiyama, T.; Shirakawa, E. *Top. Curr. Chem.* **2002**, *219*, 61–85. (i) Komiya, T.; Minami, Y.; Hiyama, T. *ACS Catal.* **2017**, *7*, 631–651.
- (2) (a) Marciniak, B.; Maciejewski, H.; Pietraszuk, C.; Pawluc, P. Hydrosilylation of Alkynes and their derivatives. In *Hydrosilylation. A Comprehensive Review of Recent Advances*; Marciniak, B., Ed.; Springer: Berlin, 2009; Advances in Silicon Science. (b) Roy, A. K. *Adv. Organomet. Chem.* **2007**, *55*, 1–59. (c) Lim, D. S. W.; Anderson, E. A. *Synthesis* **2012**, *44*, 983–1010. (d) Trost, B. M.; Ball, Z. T. *Synthesis* **2005**, *2005*, 853–887.
- (3) For selected examples, see: (a) Doyle, M. P.; High, K. G.; Nesloney, C. L.; Clayton, T. W.; Lin, J. *Organometallics* **1991**, *10*, 1225–1226. (b) Lewis, L. N.; Sy, K. G.; Bryant, G. L.; Donahue, P. E. *Organometallics* **1991**, *10*, 3750–3759. (c) Murphy, J. P.; Spencer, J. L.; Procter, G. *Tetrahedron Lett.* **1990**, *31*, 1051–1054. (d) Kyoko, T.; et al. *Tetrahedron Lett.* **1993**, *34*, 8263–8266. (e) Denmark, S. E.; Wang, Z. *Org. Lett.* **2001**, *3*, 1073–1076. (f) Itami, K.; Mitsudo, K.; Nishino, A.; Yoshida, J. *J. Org. Chem.* **2002**, *67*, 2645–2652. (g) Blug,

- M.; Le Goff, X.-F.; Mézailles, N.; Le Floch, P. *Organometallics* **2009**, *28*, 2360–2362. (h) Wu, W.; Li, C.-J. *Chem. Commun.* **2003**, 1668–1669. (i) Aneetha, H.; Wu, W.; Verkade, J. G. *Organometallics* **2005**, *24*, 2590–2596. (j) De Bo, G.; Berthon-Gelloz, G.; Tinant, B.; Markó, I. E. *Organometallics* **2006**, *25*, 1881–1890. (k) Berthon-Gelloz, G.; Schumers, J.-M.; De Bo, G.; Markó, I. E. *J. Org. Chem.* **2008**, *73*, 4190–4197. (l) Silbestri, G. F.; Flores, J. C.; de Jesús, E. *Organometallics* **2012**, *31*, 3355–3360. (m) Ortega-Moreno, L.; Peloso, R.; Maya, C.; Suárez, A.; Carmona, E. *Chem. Commun.* **2015**, *51*, 17008–17011. (n) Dierick, S.; Vercruyse, E.; Berthon-Gelloz, G.; Markó, I. E. *Chem. - Eur. J.* **2015**, *21*, 17073–17078.

(4) For examples of selective β -(Z)-vinylsilane formation with Ru catalysts, see: (a) Esteruelas, M. A.; Herrero, J.; Oro, L. A. *Organometallics* **1993**, *12*, 2377–2379. (b) Na, Y.; Chang, S. *Org. Lett.* **2000**, *2*, 1887–1889. (c) Katayama, H.; Taniguchi, K.; Kobayashi, M.; Sagawa, T.; Minami, T.; Ozawa, F. *J. Organomet. Chem.* **2002**, *645*, 192–200. (d) Nagao, M.; Asano, K.; Umeda, K.; Katayama, H.; Ozawa, F. *J. Org. Chem.* **2005**, *70*, 10511–10514. (e) Maifeld, S. V.; Tran, M. N.; Lee, D. *Tetrahedron Lett.* **2005**, *46*, 105–108. (f) Gao, R.; Pahl, D. R.; Cundari, T. R.; Yi, C. S. *Organometallics* **2014**, *33*, 6937–6944. (g) Conifer, C.; Gunanathan, C.; Rinesch, T.; Hölscher, M.; Leitner, W. *Eur. J. Inorg. Chem.* **2015**, *2015*, 333–339.

(5) For α -selective Ru catalysts, see: (a) Trost, B. M.; Ball, Z. T. *J. Am. Chem. Soc.* **2001**, *123*, 12726–12727. (b) Kawanami, Y.; Sonoda, Y.; Mori, T.; Yamamoto, K. *Org. Lett.* **2002**, *4*, 2825–2827. (c) Trost, B. M.; Ball, Z. T. *J. Am. Chem. Soc.* **2005**, *127*, 17644–17655.

(6) For selected examples, see: (a) Tanke, R. S.; Crabtree, R. H. *J. Am. Chem. Soc.* **1990**, *112*, 7984–7989. (b) Jun, C.-H.; Crabtree, R. H. *J. Organomet. Chem.* **1993**, *447*, 177–187. (c) Esteruelas, M. A.; Oliván, M.; Oro, L. A. *Organometallics* **1996**, *15*, 814–822. (d) Vicent, C.; Viciano, M.; Mas-Marzá, E.; Sanaú, M.; Peris, E. *Organometallics* **2006**, *25*, 3713–3720. (e) Miyake, Y.; Isomura, E.; Iyoda, M. *Chem. Lett.* **2006**, *35*, 836–837. (f) Sridevi, V. S.; Fan, W. Y.; Leong, W. K. *Organometallics* **2007**, *26*, 1157–1160. (g) Iglesias, M.; Sanz Miguel, P. J.; Polo, V.; Fernández-Álvarez, F. J.; Pérez-Torrente, J. J.; Oro, L. A. *Chem. - Eur. J.* **2013**, *19*, 17559–17566. (h) Pérez-Torrente, J. J.; Nguyen, D. H.; Jiménez, M. V.; Modrego, F. J.; Puerta-Oteo, R.; Gómez-Bautista, D.; Iglesias, M.; Oro, L. A. *Organometallics* **2016**, *35*, 2410–2422.

(7) (a) Takeuchi, R.; Tanouchi, N. *J. Chem. Soc., Chem. Commun.* **1993**, 1319–1320. (b) Takeuchi, R.; Tanouchi, N. *J. Chem. Soc., Perkin Trans. 1* **1994**, 2909–2913.

(8) Faller, J. W.; D'Alliessi, D. G. *Organometallics* **2002**, *21*, 1743–1746 and references therein.

(9) Sato, A.; Kinoshita, H.; Shinokubo, H.; Oshima, K. *Org. Lett.* **2004**, *6*, 2217–2220.

(10) (a) Takeuchi, R.; Nitta, S.; Watanabe, D. *J. Chem. Soc., Chem. Commun.* **1994**, 1777–1778. (b) Takeuchi, R.; Nitta, S.; Watanabe, D. *J. Org. Chem.* **1995**, *60*, 3045–3051. (c) Takeuchi, R.; Ebata, I. *Organometallics* **1997**, *16*, 3707–3710.

(11) Ojima, I.; Clos, N.; Donovan, R. J.; Ingallina, P. *Organometallics* **1990**, *9*, 3127–3133 and references therein.

(12) (a) Mori, A.; Takahisa, E.; Kajiro, H.; Nishihara, K.; Hiyama, T. *Chem. Lett.* **1998**, *27*, 443–444. (b) Mori, A.; Takahisa, E.; Yamamura, Y.; Kato, T.; Mudalige, A. P.; Kajiro, H.; Hirabayashi, K.; Nishihara, Y.; Hiyama, T. *Organometallics* **2004**, *23*, 1755–1765.

(13) (a) Andavan, G. T. S.; Bauer, E. B.; Letko, C. S.; Hollis, T. K.; Tham, F. S. *J. Organomet. Chem.* **2005**, *690*, 5938–5947. (b) Rivera, G.; Elizalde, O.; Roa, G.; Montiel, I.; Bernès, S. *J. Organomet. Chem.* **2012**, *699*, 82–86. (c) Huckaba, A. J.; Hollis, T. K.; Howell, T. O.; Valle, H. U.; Wu, Y. *Organometallics* **2013**, *32*, 63–69.

(14) (a) Hill, J. E.; Nile, T. A. *J. Organomet. Chem.* **1977**, *137*, 293–300. (b) Lappert, M. F.; Maskell, R. K. *J. Organomet. Chem.* **1984**, *264*, 217–228. (c) Zeng, J. Y.; Hsieh, M.-H.; Lee, H. M. *J. Organomet. Chem.* **2005**, *690*, 5662–5671. (d) Poyatos, M.; Mas-Marzá, E.; Mata, J. A.; Sanaú, M.; Peris, E. *Eur. J. Inorg. Chem.* **2003**, *2003*, 1215–1221. (e) Mas-Marzá, E.; Poyatos, M.; Sanaú, M.; Peris, E. *Inorg. Chem.* **2004**, *43*, 2213–2219. (f) Poyatos, M.; Maise-François, A.; Bellemin-Lapponnaz, S.; Gade, L. H. *Organometallics* **2006**, *25*, 2634–2641.

(g) Viciano, M.; Mas-Marzá, E.; Sanaú, M.; Peris, E. *Organometallics* **2006**, *25*, 3063–3069. (h) Iglesias, M.; Aliaga-Lavrijsen, M.; Sanz Miguel, P. J.; Fernández-Álvarez, F. J.; Pérez-Torrente, J. J.; Oro, L. A. *Adv. Synth. Catal.* **2015**, *357*, 350–354.

(15) Mas-Marzá, E.; Sanaú, M.; Peris, E. *Inorg. Chem.* **2005**, *44*, 9961–9967.

(16) (a) Jiménez, M. V.; Pérez-Torrente, J. J.; Bartolomé, M. I.; Gierz, V.; Lahoz, F. J.; Oro, L. A. *Organometallics* **2008**, *27*, 224–234. (b) Busetto, L.; Cassani, M. C.; Femoni, C.; Mancinelli, M.; Mazzanti, A.; Mazzoni, R.; Solinas, G. *Organometallics* **2011**, *30*, 5258–5272. (c) Cassani, M. C.; Brucka, M. A.; Femoni, C.; Mancinelli, M.; Mazzanti, A.; Mazzoni, R.; Solinas, G. *New J. Chem.* **2014**, *38*, 1768–1779. (d) Mancano, G.; Page, M. J.; Bhadbhade, M.; Messerle, B. A. *Inorg. Chem.* **2014**, *53*, 10159–10170. (e) Diachenko, V.; Page, M. J.; Gatus, M. R. D.; Bhadbhade, M.; Messerle, B. *Organometallics* **2015**, *34*, 4543–4552.

(17) (a) Ishikawa, Y.; Yamamoto, Y.; Asao, N. *Catal. Sci. Technol.* **2013**, *3*, 2902–2905. (b) Caporusso, A. M.; Aronica, L. A.; Schiavi, E.; Martra, G.; Vitulli, G.; Salvadori, P. J. *Organomet. Chem.* **2005**, *690*, 1063–1066. (c) Psyllaki, A.; Lykakis, I. N.; Stratakis, M. *Tetrahedron* **2012**, *68*, 8724–8731.

(18) (a) Mo, Z.; Xiao, J.; Gao, Y.; Deng, L. *J. Am. Chem. Soc.* **2014**, *136*, 17414–17417. (b) Guo, J.; Lu, Z. *Angew. Chem., Int. Ed.* **2016**, *55*, 10835–10838.

(19) Field, L. D.; Ward, A. J. *J. Organomet. Chem.* **2003**, *681*, 91–97.

(20) Goldberg, Y.; Alper, H. *J. Chem. Soc., Chem. Commun.* **1994**, 1209–1210.

(21) (a) Hopkinson, M. N.; Richter, C.; Schedler, M.; Glorius, F. *Nature* **2014**, *510*, 485–496. (b) Díez-González, S.; Marion, N.; Nolan, S. P. *Chem. Rev.* **2009**, *109*, 3612–3676.

(22) (a) Wang, C.-Y.; Liu, Y.-H.; Peng, S.-M.; Liu, S.-T. *J. Organomet. Chem.* **2006**, *691*, 4012–4020. (b) Warsink, S.; van Aubel, C. M. S.; Weigand, J. J.; Liu, S.-T.; Elsevier, C. J. *Eur. J. Inorg. Chem.* **2010**, *2010*, 5556–5562. (c) Cao, C.; Sun, R.; Chen, Q.; Lv, L.; Shi, Y.; Pang, G. *Transition Met. Chem.* **2013**, *38*, 351–358.

(23) (a) Garrison, J. C.; Youngs, W. J. *Chem. Rev.* **2005**, *105*, 3978–4008. (b) Lin, I. J. B.; Vasam, C. S. *Coord. Chem. Rev.* **2007**, *251*, 642–670.

(24) Yu, X.-Y.; Patrick, B. O.; James, B. R. *Organometallics* **2006**, *25*, 2359–2363 and references therein.

(25) Braunstein, P.; Naud, F. *Angew. Chem., Int. Ed.* **2001**, *40*, 680–699 and references therein.

(26) (a) Gründemann, S.; Albrecht, M.; Loch, J. A.; Faller, J. W.; Crabtree, R. H. *Organometallics* **2001**, *20*, 5485–5488. (b) Miecznikowski, J. R.; Gründemann, S.; Albrecht, M.; Mégret, C.; Clot, E.; Faller, J. W.; Eisenstein, O.; Crabtree, R. H. *Dalton Trans.* **2003**, 831–838. (c) Hernández-Juárez, M.; López-Serrano, J.; Lara, P.; Morales-Cerón, J. P.; Vaquero, M.; Álvarez, E.; Salazar, V.; Suárez, A. *Chem. - Eur. J.* **2015**, *21*, 7540–7555.

(27) Wang, C.-Y.; Fu, C.-F.; Liu, Y.-H.; Peng, S.-M.; Liu, S.-T. *Inorg. Chem.* **2007**, *46*, 5779–5786.

(28) For comparison with other catalytic systems, the reaction of phenylacetylene with Et₃SiH was also carried out. Catalytic activity and selectivity identical with those for the reaction with ¹⁸Pr₃SiH were observed.

(29) For selected examples of the influence of the steric hindrance of hemilabile ligand fragments on selectivity, see: (a) Khlebnikov, V.; Meduri, A.; Mueller-Bunz, H.; Montini, T.; Fornasiero, P.; Zangrando, E.; Milani, B.; Albrecht, M. *Organometallics* **2012**, *31*, 976–986. (b) Warsink, S.; Chang, I.-H.; Weigand, J. J.; Hauwert, P.; Chen, J.-T.; Elsevier, C. J. *Organometallics* **2010**, *29*, 4555–4561. (c) Flapper, J.; van Leeuwen, P. W. N. M.; Elsevier, C. J.; Kamer, P. C. J. *Organometallics* **2009**, *28*, 3264–3271.

(30) Lukevics, E.; Dzintara, M. *J. Organomet. Chem.* **1985**, *295*, 265–315.

(31) Chalk, A. J.; Harrod, J. F. *J. Am. Chem. Soc.* **1965**, *87*, 16–21.

(32) (a) Tabata, M.; Yang, W.; Yokota, K. *Polym. J.* **1990**, *22*, 1105–1107. (b) Amer, I.; Schumann, H.; Ravindar, V.; Baidossi, W.; Goren, N.; Blum, J. *J. Mol. Catal.* **1993**, *85*, 163–171. (c) Kishimoto, Y.;

Eckerle, P.; Miyatake, T.; Ikariya, T.; Noyori, R. *J. Am. Chem. Soc.* **1994**, *116*, 12131–12132. (d) Kishimoto, Y.; Miyatake, T.; Ikariya, T.; Noyori, R. *Macromolecules* **1996**, *29*, 5054–5055.

(33) (a) Gómez-Gallego, M.; Sierra, M. A. *Chem. Rev.* **2011**, *111*, 4857–4963. (b) Simmons, E. M.; Hartwig, J. F. *Angew. Chem., Int. Ed.* **2012**, *51*, 3066–3072.